

# Diblock Copolymer Ordering Induced by Patterned Surfaces above the Order–Disorder Transition

Yoav Tsori and David Andelman\*

School of Physics and Astronomy, Raymond and Beverly Sackler Faculty of Exact Sciences, Tel Aviv University, 69978 Ramat Aviv, Israel

Received July 14, 2000; Revised Manuscript Received November 27, 2000

**ABSTRACT:** We investigate the morphology of diblock copolymers in the vicinity of flat, chemically patterned surfaces. We use a Ginzburg–Landau free energy to describe the spatial variations of the order parameter in terms of a general two-dimensional surface pattern above the order–disorder transition. The propagation of several surface patterns into the bulk is investigated. The oscillation period and decay length of the surface Fourier modes are calculated in terms of system parameters. We show that two parallel surfaces having simple one-dimensional patterns can induce a complex three-dimensional copolymer structure between them. Lateral order is observed parallel to a patterned surface as a result of order perpendicular to the surface. Surfaces which have a finite chemical pattern size (e.g., a stripe of finite width) induce lamellar ordering extending into the bulk. Close to the surface pattern the lamellae are strongly perturbed as they try to adjust to the surface pattern.

## I. Introduction

The bulk properties of diblock copolymers (BCP) are by now well understood.<sup>1–5</sup> These long linear macromolecules composed of two incompatible subchains, or blocks, cannot phase separate because of the covalent bond between the two blocks. This connectivity, together with the incompatibility between the two blocks, gives rise to the appearance of microphase separated phases. The state of segregation is controlled by  $N\chi$  and  $f$ , where  $\chi$  is the Flory parameter,  $N = N_A + N_B$  is the total number of constituent monomers per chain and  $f$  is the fraction of the A block,  $f = N_A/(N_A + N_B)$ . For large enough  $N\chi$  one of the ordered phases, lamellar, hexagonal, or cubic phases, is preferred, depending on the degree of asymmetry  $f$ .

Less understood is the interfacial behavior of copolymer melts near solid surfaces or at the free surface with air. Surface phenomena of BCP may enable creating and controlling technologically important devices of characteristic size comparable to the wavelength of light. As examples we mention waveguides, light-emitting diodes, and other optoelectronic devices, antireflection coatings for optical surfaces,<sup>6</sup> and dielectric mirrors.<sup>7</sup>

The presence of a wall in a BCP system leads to new energy and length scales, depending on the specific chemical interactions of the polymer with the surface. In a semi-infinite system in contact with a single planar wall, the morphology near the surface can be very different from the bulk morphology. Fredrickson<sup>8</sup> has considered BCP in contact with a surface having a uniform preferential adsorption to one of the two blocks. He applied mean-field theory to a system above its order–disorder transition (ODT) and found that the order parameter (being the relative concentration between the two blocks) has decaying oscillations. He showed that the oscillation periodicity depends on  $\chi$ , and tends to the bulk lamellar periodicity as  $\chi \rightarrow \chi_c$ . In the same  $\chi \rightarrow \chi_c$  limit, the correlation length  $\xi$  of the oscillations was found to diverge. Further investigations<sup>9</sup> showed that the inclusion of higher order, nonlinear corrections to the mean-field theory results in a nondiverging  $\xi$ . For the same system cooled below the

ODT, modulated sinusoidal behavior was found. In a related work<sup>10</sup> a Ginzburg–Landau free energy was used to describe the propagation of a surface-induced lamellar ordering into a bulk hexagonal phase. In the strong-segregation limit a lamellar region of finite thickness close to the surface becomes stable, provided that the surface field is larger than some critical value.

The situation is even more complicated in thin BCP films, placed between two walls. The distance between the two walls, associated with the film thickness, can be comparable to the modulations periodicity in the bulk, but the surface-induced morphology can be of different symmetry than that of the bulk.<sup>11,12</sup> For a system taken in one of its ordered phases (below the ODT), the free energy has a local minimum when the spacing between the surfaces is an integer multiple of the bulk repeat period. Shull<sup>13</sup> has applied self-consistent field theory (SCF) to bulk and thin-film BCP. Similar SCF method has also been used<sup>14,15</sup> to study the stability of parallel, perpendicular and mixed lamellar phases in thin films of BCP. The latter mixed phase consists of parallel lamellae near one surface and perpendicular lamellae near the opposite surface, but it was found to be unstable for symmetric A–B ( $f = 1/2$ ) diblock copolymers.

So far, we mentioned situations where the surfaces have a uniform preference to one of the two blocks. More complex, chemically patterned surfaces break the lateral translation symmetry. Different surface regions will now have a different preference for the A/B blocks, thereby inducing a lateral structured morphology near the surface. Pereira and Williams<sup>16</sup> have recently investigated BCP confined by patterned surfaces below the ODT using a phenomenological free energy model. They have given expressions for the order parameter profiles as well as calculated the phase diagram of the system. The order parameter profile obtained by them is sensitive to the exact magnitude of the coefficients in their free energy.<sup>17</sup> Few works took into account the possibility of a nonuniform surface above the ODT. In particular, Petera and Muthukumar<sup>18,19</sup> have investigated the effect of a *one-dimensional* sinusoidal surface

pattern on BCP morphologies close to the surface in the weak-segregation limit, both below and above the ODT.

In this paper we consider a BCP melt above the ODT near a surface, whose pattern is truly arbitrary in two dimensions, generalizing the results of refs 18 and 19. A Ginzburg–Landau free energy, expressed in term of the polymer concentration, is presented in section II. In section III, we consider a melt close to one surface or confined between two surfaces whose chemical pattern has one-dimensional symmetry. Minimization of the free energy expansion gives rise to an Euler–Lagrange equation for the order parameter. A natural generalization to two-dimensional surface patterns is then considered in section IV. We are able to give a complete description of the order parameter in terms of all the Fourier modes of the surface pattern. Finally, conclusions and some future prospects are presented in section V.

## II. The Model

The copolymer melt is described by the order parameter  $\phi(\mathbf{r})$ , defined as  $\phi(\mathbf{r}) = \phi_A(\mathbf{r}) - f$ , the difference in local A monomer concentration from its average value. Hereafter we restrict the treatment to the symmetric  $f = 1/2$  case, following the coarse-grained free energy used by various authors<sup>20–23</sup>

$$\frac{N}{k_B T} F = \int d^3\mathbf{r} \left[ \frac{1}{2} \tau \phi^2 + \frac{1}{2} h [(\nabla^2 + q_0^2) \phi]^2 + \frac{u}{4!} \phi^4 - \mu \phi \right] \quad (1)$$

where  $k_B$  is the Boltzmann constant,  $T$  is the temperature and  $\mu$  is the chemical potential. The other parameters are

$$q_0 \approx 1.95/R_g \quad (2)$$

$$\tau = 2\rho N(\chi_c - \chi) \quad (3)$$

$$\chi_c \approx 10.49/N \quad (4)$$

$$h = 1.5\rho c^2 R_g^2/q_0^2 \quad (5)$$

The system has two fundamental length scales. The first is  $q_0^{-1}$ , the wavelength of the lamellar phase just below the ODT, expressed in eq 2 by  $R_g$ , the radius of gyration of the chains. The second length scale,  $(\tau/h)^{-1/4} = \alpha^{-1/2} (N\chi_c - N\chi)^{-1/4}$  with  $\alpha = 2q_0^2/(1.95\sqrt{3}c)$ , characterizes the decay of surface-induced modulations, and diverges close to the ODT. The chain density  $\rho$  is equal to  $1/Na^3$  for an incompressible melt, and  $u/\rho$  and  $c$  are dimensionless parameters of order unity. More details can be found in ref 22, and extensions for asymmetric BCP,  $f \neq 1/2$ , are possible as well. The use of eq 1 limits our treatment to a region of the phase diagram close enough to the critical point where the expansion in powers of  $\phi$  and its derivatives is valid, but not too close, because then critical fluctuation effects may be important.<sup>20</sup>

This and similar types of free energy has been used to describe bulk and surface phenomena in amphiphilic systems,<sup>24</sup> diblock copolymers,<sup>3,4,22,25–27</sup> Langmuir films<sup>28</sup> and magnetic (garnet) films.<sup>29</sup> The  $\phi^2$  and  $\phi^4$  terms appear in the usual Landau expansion. The added  $\phi\nabla^2\phi$  and  $(\nabla^2\phi)^2$  terms compete to produce *modulated phases* below the order–disorder temperature. This free energy

describes a system in the disordered phase ( $\phi = 0$ ,  $f = 1/2$ ) for  $\chi < \chi_c$  and one in the lamellar phase for  $\chi > \chi_c$ . The  $q = q_0$  mode goes critical first, and the lamellar phase is described by  $\phi = \phi_q \cos(\mathbf{q}_0 \cdot \mathbf{r})$ , of repeat period  $d_0 \equiv 2\pi/q_0$ . This single-mode approximation is accurate to order  $(\chi - \chi_c)^{1/2}$  and can be justified near the critical point.<sup>8</sup> Far from the critical point higher harmonics are needed to describe the lamellar phase. As the asymmetry in composition is increased  $|f - 1/2| > 0$ , other ordered phases of hexagonal and cubic symmetries become more stable than the lamellar phase.<sup>30</sup>

As stated above, block copolymers exhibit complex surface behavior characterized by the strength and range of the interaction between the polymer chains and the surface, the typical size of chemical heterogeneities of the surface, and the distance between the two surfaces, in the case of a thin film.

The presence of chemically interacting confining walls is modeled by adding a short-range surface coupling term in the free energy

$$F_s = \int d^2\mathbf{r}_s (\sigma(\mathbf{r}_s)\phi(\mathbf{r}_s) + \tau_s\phi^2(\mathbf{r}_s)) \quad (6)$$

The vector  $\mathbf{r}_s$  defines the position of the confining surfaces. The  $\sigma\phi$  term expresses the preferential interaction of the surface with the A and B blocks. For example, if  $\sigma > 0$ , then the B block ( $\phi < 0$ ) is attracted to the surface more than the A block ( $\phi > 0$ ). Control over the specificity of this surface term can be achieved by coating the substrate with carefully prepared random copolymers.<sup>31,32</sup> The coefficient of the  $\phi^2$  term in eq 6,  $\tau_s$ , is a surface correction to the Flory parameter  $\chi$ ,<sup>8,9,33</sup> where  $\tau_s > 0$  corresponds to a suppression of surface segregation of the A and B monomers.

We first consider systems in which the polymer melt is confined by a flat, rigid wall at  $y = 0$ , with the  $x$ -axis chosen in the plane of the wall, and is translational invariant along the  $z$ -direction. Extension to the system of two parallel surfaces located at  $y = \pm L$  is straightforward and will be considered later. The order parameter  $\phi$  is expected to vanish in regions where the interfacial interactions can be neglected

$$\lim_{y \rightarrow \infty} \phi(x, y) = 0 \quad (7)$$

recovering the value  $\phi = 0$  of the bulk phase far from the surface. In the next section we find profile solutions  $\phi(x, y)$  for a BCP system at temperatures above the bulk ODT.

## III. One Dimensional Surface Patterns

For high enough temperatures, or equivalently, for  $\chi < \chi_c$ , the stable phase is the homogeneous disordered phase, with  $\phi(\mathbf{r}) = 0$  in the bulk. The presence of a patterned surface induces ordering in the copolymer melt. If the chemical surface composition is uniform, one of the monomers, A or B, will be attracted to the surface, resulting in a parallel orientation of the lamellae (a perpendicular orientation of the chains). If the pattern is modulated, e.g., sinusoidally, then different blocks are attracted to different regions of the surface. We will start with the case of a semi-infinite system bounded by one rigid, flat surface, and then proceed to describe thin film systems between two surfaces.

**A. One Patterned Surface.** Consider the semi-infinite BCP melt occupying the  $y > 0$  half space bounded by a flat surface at  $y = 0$ . We assume a one-

dimensional periodic surface pattern and write it in terms of the Fourier components of the surface field  $\sigma(x)$

$$\sigma(x) = \sum_q \sigma_q e^{iqx} \quad (8)$$

where  $\sigma_q$  set the amplitude of the respective  $q$ -mode. The order parameter  $\phi(x,y)$  satisfies the boundary conditions on the surface and approaches the bulk solution far from the surface. It is convenient to decompose  $\phi$  in terms of its  $q$ -modes in the  $x$ -direction

$$\phi(x,y) = \sum_q f_q(y) e^{iqx} \quad (9)$$

The requirement eq 7 leads to the bulk boundary condition

$$\lim_{y \rightarrow \infty} f_q(y) = 0 \quad (10)$$

The form of  $\phi$  in eq 9 is substituted in eq 1. Above the order-disorder transition (ODT) temperature, the theory is stable to second order in  $\phi$ , and therefore the  $\phi^4$  term is neglected. Using the explicit  $x$  dependence of  $\phi$  in eq 9, we perform the  $x$  and  $z$  integration, yielding the free energy  $F$

$$F = \int \sum_q \left\{ \frac{1}{2} (\tau + hq_0^4) f_q f_q^* + hq_0^2 f_q (f_q'' - q^2 f_q)^* + \frac{1}{2} h (f_q'' - q^2 f_q) (f_q'' - q^2 f_q)^* - \mu f_q \delta_{q,0} \right\} dy + \sum_q [\sigma_q f_q^*(0) + \tau_s f_q(0) f_q^*(0)] \quad (11)$$

where (...) indicates complex conjugation (c.c.) operation. A standard minimization technique is carried on and yields the governing linear ordinary differential equation for the functions  $f_q$  for  $y > 0$ :

$$(\tau/h + (q^2 - q_0^2)^2) f_q + 2(q_0^2 - q^2) f_q'' + f_q'''' = 0 \quad (12)$$

This equation has four independent solutions in the form of an exponential  $e^{-k_q y}$ , with  $k_q$  found from the characteristic equation

$$(\tau/h + (q^2 - q_0^2)^2) + 2(q_0^2 - q^2) k_q^2 + k_q^4 = 0 \quad (13)$$

Thus, with the semi-infinite geometry, the solution is

$$f_q(y) = A_q e^{-k_q y} + B_q e^{-k_q^* y} \quad (14)$$

and

$$\begin{aligned} k_q^2 &= q^2 - q_0^2 + i(\tau/h)^{1/2} \\ &= q^2 - q_0^2 + i\alpha(N\chi_c - N\chi)^{1/2} \end{aligned} \quad (15)$$

For the numerical calculations presented below we choose the following values of parameters:  $c = 1$ ,  $N = 100$ ,  $\rho = 1/(Na^3)$ , and  $R_g = N^{1/2}a$ . In addition, the monomer length is set as the unit length ( $a = 1$ ) and all lengths are expressed in terms of  $d_0 = 2\pi/q_0$ . Substituting these values as well as the parameter values given after eq 5 yields  $\alpha \approx 0.59q_0^2$ . Each  $q$ -mode solution  $f_q$  is determined by two complex amplitudes  $\{A_q, B_q\}$ . From the solutions of eq 13, the  $k_q$  wavevectors with

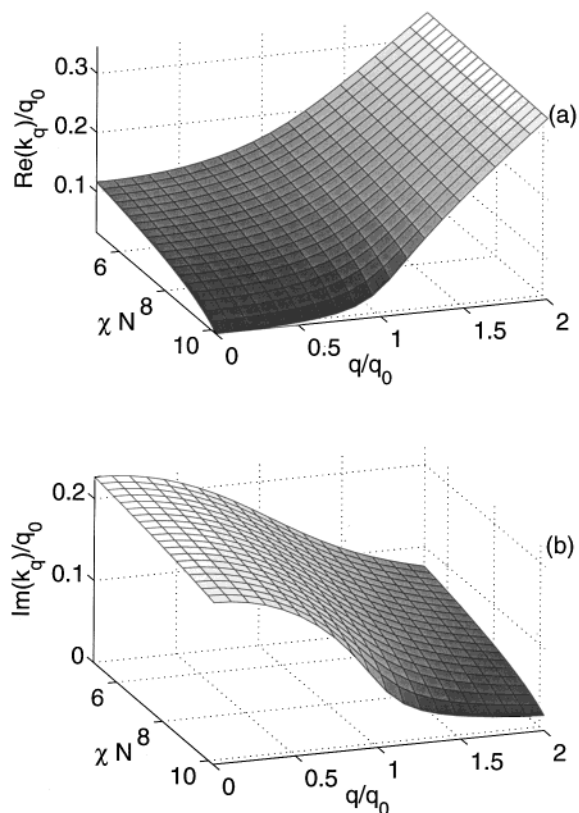


**Figure 1.** Real (a) and imaginary (b) parts of the wavevector  $k_q$  as a function of the modulation  $q$ -mode and the Flory parameter  $N\chi$ . For values of  $N\chi$  close to its critical value,  $N\chi_c \approx 10.49$ , and for small  $q$ ,  $\text{Re}(k_q)$  is small. As  $q$  increases,  $\text{Re}(k_q)$  starts to increase rapidly and  $\text{Im}(k_q)$  decreases. The value and magnitude of this sharp change in  $k_q$  are determined by the proximity to ODT. Farther from the critical point (smaller  $\chi < \chi_c$ ) the variation of  $k_q$  with  $q$  diminishes. The values of all parameters used in this and the following figures are given in the text after eq 5.

negative real value,  $\text{Re}(k_q) < 0$ , are discarded, to comply with the boundary condition, eq 10. Note that  $\text{Re}(k_q)$  increases monotonically as a function of  $q$ . A large value of  $\text{Re}(k_q)$  means short decay length, and hence the smallest surface  $q$ -mode has the largest decay length. This behavior is demonstrated in Figure 1 showing the  $q$  and  $\chi$  dependence of the real and imaginary parts of the wavevector  $k_q$ . For a fixed value of  $\chi$ , the decay length, which is proportional to  $1/\text{Re}(k_q)$ , decreases as  $q$  increases, while the wavelength  $2\pi/\text{Im}(k_q)$  of the modulations in  $f_q(y) \sim e^{-k_q y}$  increases.

The boundary conditions for the functions  $f_q$  can be determined by considering the Euler-Lagrange equation for  $f_q$  in the range that includes  $y = 0$ . There are two conditions relating  $f_q$  and its derivatives at  $y = 0$ :

$$(q_0^2 - q^2) f_q(0) + f_q''(0) = 0 \quad (16)$$

$$\frac{\sigma_q}{h} + \frac{2\tau_s}{h} f_q(0) + (q_0^2 - q^2) f_q'(0) + f_q'''(0) = 0 \quad (17)$$

The  $q = 0$  surface mode is the only mode which does not average to zero, and for this mode the condition  $\int f_0 dy = 0$  replaces eq 16. Recently, it has been found<sup>34</sup> that BCP morphologies can be induced by a surface even in the absence of a chemical field  $\sigma$ . This effect can be attributed to a loss of entropy close to the surfaces. However, in our linear theory this does not happen, and

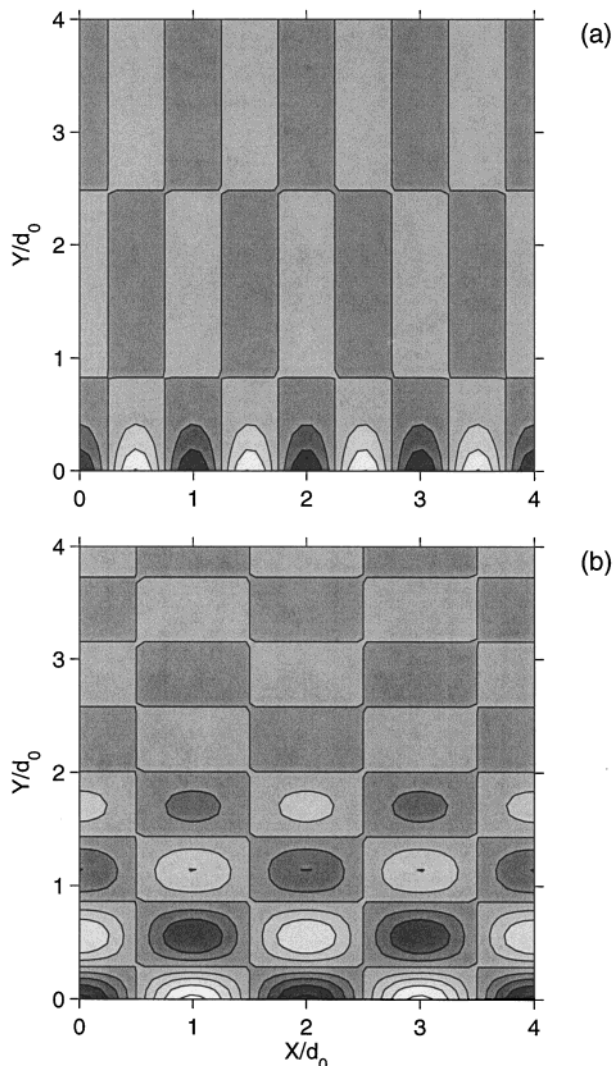


**Figure 2.** Contour plot of the BCP order parameter  $\phi(x,y)$ , where the surface pattern (bottom line,  $y = 0$ ) contains only one mode:  $\sigma(x) = \sigma_q \cos(qx)$ , with  $\sigma_q = 1$ . A-rich regions (light) are separated from B-rich regions (dark) by eight gray scales. In part a,  $q = q_0$  while in part b  $q = 0.5q_0$ . The decay length  $\xi$  is smaller in part a than in part b because the surface  $q$  mode is larger. The Flory parameter was set to  $N\chi = 10.4 < N\chi_c$ . All lengths are scaled by the natural lamellar period  $d_0 = 2\pi/q_0$ . For simplicity, it is assumed here and in the following figures that the Flory parameter does not change at the surface,  $\tau_s = 0$ .

the copolymer response is proportional to the field  $\sigma$ . The case where  $\sigma_0$  is a nonzero constant and  $\sigma_{q \neq 0} = 0$  corresponds to the special case of uniform interfacial interactions as discussed in refs 8, 11, and 12. The system exhibits a decaying lamellar layering of the polymers, with the B-polymer adsorbed to the surface if  $\sigma_0 > 0$ .

Close to the ODT, the complex wavevector  $k_0$  can be approximated by

$$k_0 \approx \frac{\alpha}{2q_0} (N\chi_c - N\chi)^{1/2} + iq_0 \left( 1 - \alpha^2 \frac{N\chi_c - N\chi}{8q_0^4} \right) \quad (18)$$

This expression shows that  $f_0 \sim e^{-k_0 y} \sim e^{-y/\xi}$  has a diverging characteristic length  $\xi \sim (\chi_c - \chi)^{-1/2}$ , while the oscillatory part has a wavelength slightly longer than that of the bulk lamellar phase, in agreement with the results of Fredrickson for chemically uniform sur-

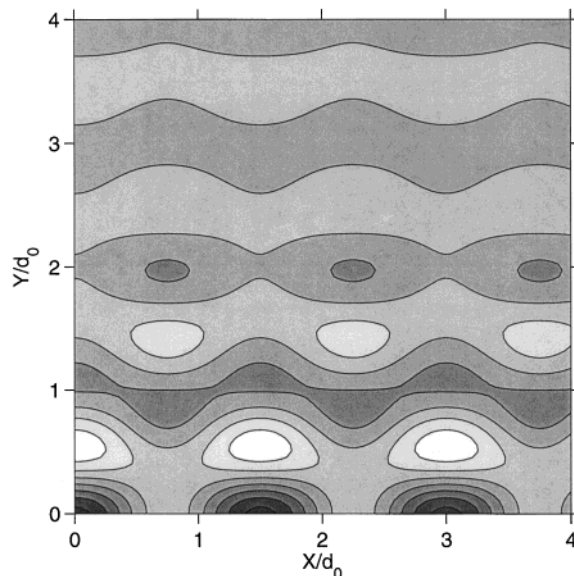


**Figure 3.** Contour plot of the BCP order parameter close to the critical point ( $N\chi = 10.4$ ). The surface pattern at  $y = 0$  is  $\sigma(x) = \sigma_0 + \sigma_q \cos(qx)$ , where  $\sigma_0$  is the average preference,  $q = 2/3q_0$ , and the amplitudes are  $\sigma_0 = \sigma_q = 0.1$ . The  $q = 0$  surface mode has a longer range effect than the  $q > 0$  surface mode, and induces parallel lamellar arrangement farther away from the surface. At yet larger distances, the order parameter decays to its bulk  $\phi = 0$  value.

faces.<sup>8</sup> As a result of the assumed short-range surface interactions, the periodicity and decay length of  $f_q$  depend only on properties of the bulk, and not on surface details.

Using the boundary conditions eq 16 and eq 17 the amplitude of the exponential oscillations is found to obey

$$A_q = \frac{-\sigma_q}{4\tau_s + 2\text{Im}(k_q)\sqrt{h\tau}} \quad (19)$$

and it may diverge even above the ODT if the surface orders at a higher temperature than the bulk,  $\tau_s < 0$ . In the case where the surface orders at the same temperature as the bulk,  $\tau_s = 0$ , the  $q$ -mode amplitude  $A_q$  diverges as  $\tau^{-1/2} \sim (\chi_c - \chi)^{-1/2}$ .

An interesting limit occurs when  $\sigma_0 = 0$ , that is, when the average surface interaction is zero (no net adsorption). No lamellar ordering parallel to the surface is expected. Indeed, the resulting checkerboard behavior is illustrated for a surface pattern chosen for simplicity to contain only one mode:  $\sigma(x) = \sigma_q \cos(qx)$ . Figure 2 depicts alternating A-rich (white) and B-rich (black) regions. In a the decay length  $\xi$  is smaller than in b, because in the former case the surface periodicity  $2\pi/q$  is twice as large. The oscillatory behavior, characterized by  $\text{Im}(k_q)$ , has a very long wavelength, diverging as  $(\chi_c - \chi)^{-1/2}$  close to the ODT point.

Usually, if no special measures are taken,<sup>31,32</sup> there is a net preference of the surface for one of the monomers:  $\sigma_0 \neq 0$ . The BCP morphology where the surface interactions were chosen to have both a nonzero average preference and undulatory character, namely  $\sigma = \sigma_0 + \sigma_q \cos(qx)$ , is shown in Figure 3. A smooth crossover from surface-induced ordering at small distance to the bulk disorder occurs. The parallel lamellae resulting from the  $\sigma_0$  term persist farther from the surface than the bulges resulting from the  $\sigma_q$  term, as  $f_0$  decays slower than  $f_q$ . For a given  $\sigma_0$ , having a higher

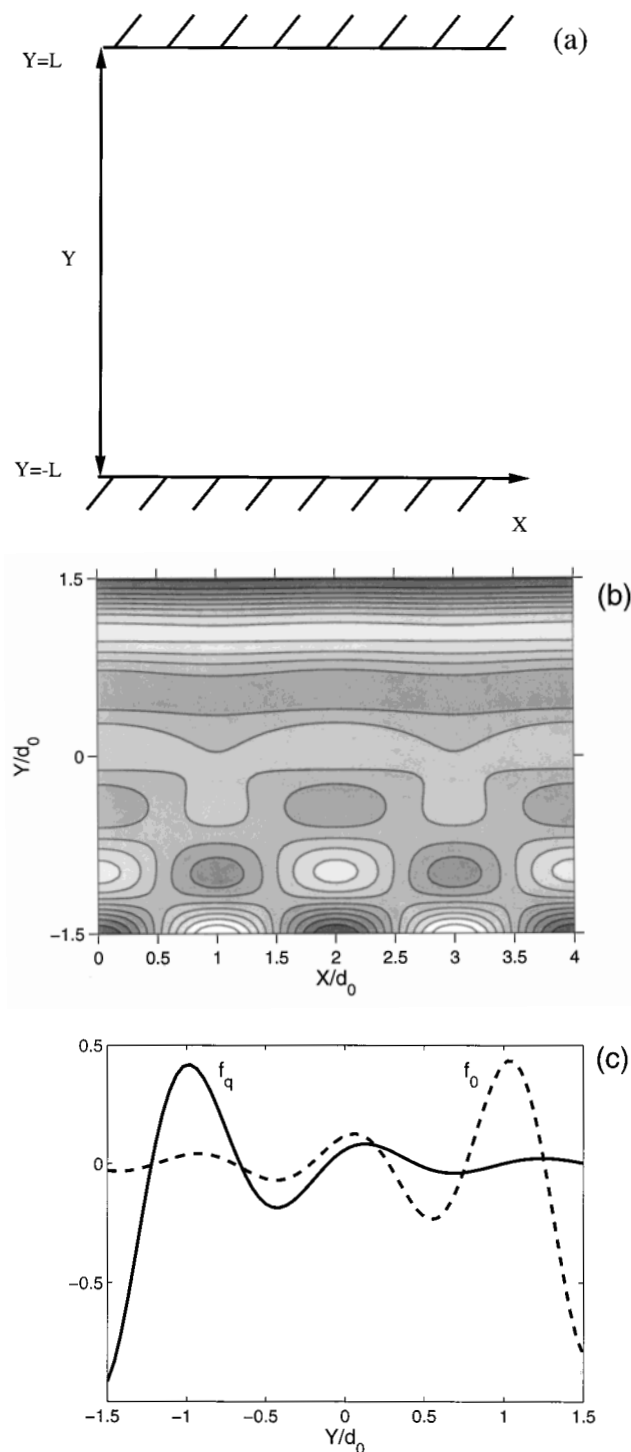


**Figure 4.** (a) Sketch of a thin-film system confined between two surfaces. The  $y$  axis is perpendicular to the two parallel surfaces, located at  $y = \pm L$ . The  $z$  axis is out of the plane of the paper. (b) Thin BCP film between two surfaces. The top one at  $y = L = 1.5d_0$  is homogeneous,  $\sigma^+(x) = 0.1$  the bottom one at  $y = -L$  is oscillatory,  $\sigma^-(x) = 0.1 \cos(qx)$ , and  $q$  is chosen to be  $q = q_0/2$ . As expected, the B polymer (shown in dark) is preferentially attracted to the upper surface, while the bottom surface exhibits modulated adsorption pattern. This pattern propagates to the top surface. The Flory parameter was chosen as  $N\chi = 10$ . (c) The two amplitudes  $f_0(y)$  (dashed line) and  $f_q(y)$  (solid line) from Figure 4b plotted against  $y/d_0$ .  $f_0$  is negative at  $y = L$  (top uniform surface of part b), and  $f_q$  is negative at the opposite modulated surface,  $y = -L$ . Notice that the pattern at  $y = -L$  induces order at the vicinity of the other surface, as  $f_q(L) \neq 0$ , although  $\sigma^+ = \text{constant}$ . The surface  $q$ -mode is  $q = q_0/2$  and the Flory parameter is  $N\chi = 10$  as in part b.

$q$ -mode or reducing the modulation strength  $\sigma_q$  will enhance the lamellar features far from the surface.

**B. Two Patterned Surfaces.** Until now the BCP melt was assumed to be bounded by one surface at  $y = 0$ . In this section we extend our analysis to a thin-film system confined between two parallel surfaces located at  $y = L$  and  $y = -L$ , shown schematically in Figure 4a. When the distance  $2L$  between the surfaces is comparable to the natural bulk periodicity, the two surfaces interact via the BCP and the resulting film morphology can be very different from that of the one-surface case (section III.A). However, the mathematical analysis is almost the same; one only has to apply different boundary conditions on the BCP order parameter  $\phi$ .

The surfaces at  $y = \pm L$  are assumed to carry different surface fields of the form  $\sigma^\pm(x) = \sum_q \sigma_q^\pm e^{iqx}$ . Only small modifications must be included to generalize the results of the previous section. The same ansatz eq 9 for  $\delta\phi$  is used. The functions  $f_q$  that minimize the appropriate  $x$ -averaged free energy eq 1 obey

$$f_q(y) = A_q e^{-k_q y} + B_q e^{-k_q^* y} + C_q e^{k_q y} + D_q e^{k_q^* y} \quad (20)$$

with  $\{k_q\}$  given by the same relation eq 15. However, unlike the semi-infinite case of eq 14, here both signs of the  $k_q$  vectors need to be used because the system is finite in the  $y$ -direction. In addition, the boundary conditions for  $f_q$  are

$$f_q''(\pm L) + (q_0^2 - q^2)f_q(\pm L) = 0$$

$$\frac{\sigma_q^\pm}{h} + \frac{2\tau_s}{h} f_q(\pm L) \mp (q_0^2 - q^2) f_q'(\pm L) \mp f_q'''(\pm L) = 0 \quad (21)$$

We consider now several specific surfaces. In the first,  $\sigma^+(x) = 0.1$  is a constant, while  $\sigma^-(x) = 0.1 \cos(qx)$  which has only one  $q$ -mode, is purely sinusoidal and average to zero, as depicted in Figure 4b. As expected, the B polymer (in black) is attracted to the upper surface, while the bottom surface exhibits modulated adsorption pattern. Although lamellar features are seen close to the top surface, the overall apparent phase in the sample cannot be classified as such. The corresponding plots of the functions  $f_0(y)$  and  $f_q(y)$  are shown in Figure 4c (same parameters as in Figure 4b). In general  $f_q$  is nonzero even at the  $y = L$  surface, although the surface does not induce modulations by itself as  $\sigma^+(x) = \text{constant}$ . Thus, modulations propagate from one surface to the other by the copolymer melt. This is an interesting observation which may have relevance in applications. It relies on the relatively small thickness of the BCP film.

The situation as depicted in Figure 4b represents a competition between two mechanisms. The modulated pattern at the bottom surface induces a laterally modulated pattern of the BCP, while the top surface uniform interaction induces a lamellar-like layering of the copolymers. The resulting morphology strongly depends on the modulation wavenumber. This effect is shown explicitly in Figure 5, where the top surface is uniform and the bottom is modulated, for a series of  $q/q_0$  values. The transition from a locally perpendicular (bottom patterned surface) to a locally parallel orientation (at the top uniform surface) is seen in part a, similar to the so-called T-junctions between grains of different

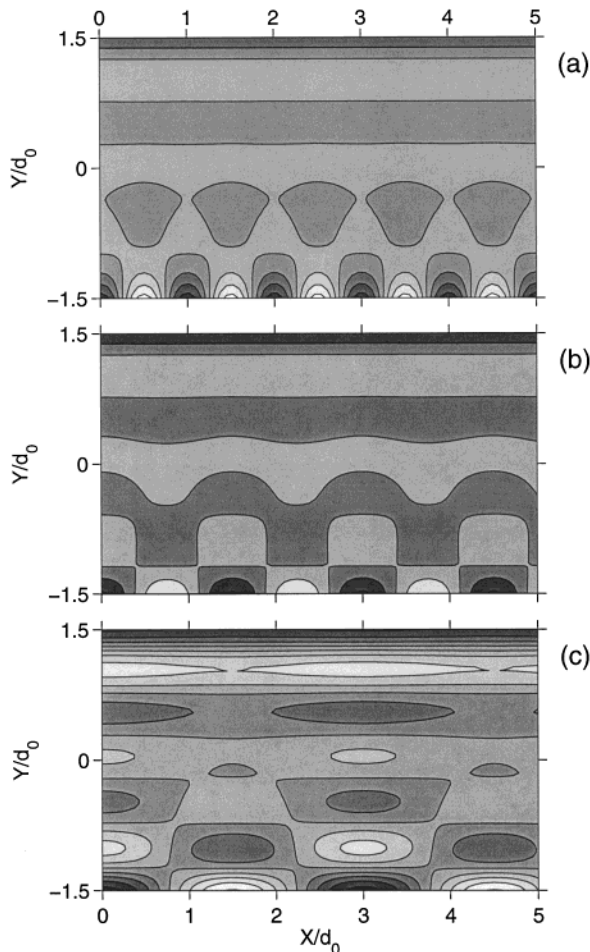


**Figure 5.** System of modulated surface  $\sigma^- = 0.1 \cos(qx)$  at  $y = -L = -1.5d_0$  and of uniform  $\sigma^+ = 0.1$  at the opposite surface,  $y = L = 1.5d_0$ , for a series of different values of  $q/q_0 = 1$  in (a),  $2/3$  in (b), and  $1/3$  in (c). The effect of changing the repeat period  $q$  is clearly seen when  $q/q_0$  varies. In all cases,  $N\chi = 10$ .

orientations.<sup>26,35</sup> Similar behavior was found by the SCF calculation in ref 19.

Figure 6a shows the spatial dependence of the BCP order parameter when the two surfaces contain only one  $q$ -mode and are patterned *in phase* with each other (symmetric arrangement), but with opposite signs,  $\sigma^\pm = \pm\sigma_q \cos(qx)$ . The copolymer patterns create a perfect checkerboard arrangement and are related to each other at the surfaces by an interchange of monomers  $A \leftrightarrow B$ . The surface pattern eq 8 contains only even  $\cos(qx)$  terms. A generalization that includes odd  $\sin(qx)$  sinusoidally varying modes is straightforward. In this case the patterns at the surfaces can be out-of-phase with each other. Figure 6b shows such a morphology, for  $\sigma^+ = \sigma_q \cos(qx)$ ,  $\sigma^- = \sigma_q \sin(qx)$ , where there is a  $\pi/2$  phase shift between the two surface fields. The perfect checkerboard arrangement of Figure 6a is now distorted as a result of this phase shift. Clearly the pattern can be distorted by adjusting also the film thickness.

#### IV. Two-Dimensional Surface Patterns

So far we considered a melt in contact with a surface or confined between two surfaces having one-dimensional symmetry. In our approximation, as in any linear response theory, there is no coupling between different  $q$ -modes proportional to  $\sigma_{q_1}\sigma_{q_2}$ . This fact allows us to

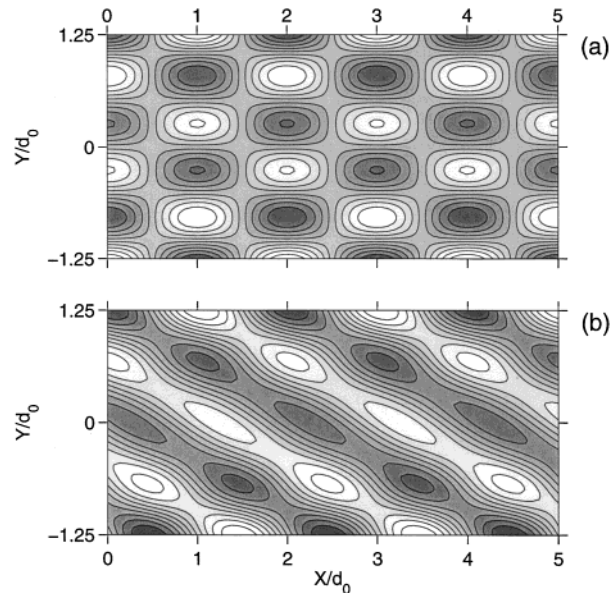


**Figure 6.** The crystalline-like checkerboard character of polymer order parameter. In part a, two patterned surfaces in phase with one another, but opposite in sign:  $\sigma^+ = -\sigma^- = \sigma_q \cos(1/2 q_0 x)$ . In part b, the patterns are  $\pi/4$  out of phase:  $\sigma^+ = \sigma_q \cos(1/2 q_0 x)$ ,  $\sigma^- = \sigma_q \sin(1/2 q_0 x)$ . The amplitude is  $\sigma_q = 0.2$ ,  $N\chi = 10.4$ , and the top and bottom surfaces are located at  $y = \pm 1.25d_0$ .

introduce a two-dimensional generalization of the surface pattern, which so far was taken to be independent of the other surface direction,  $z$ . The surface now is assumed to carry a chemical pattern  $\sigma(x, z)$  which can be written as

$$\sigma(x, y) = \sum_{q_x, q_z} \sigma_{q_x, q_z} e^{i(q_x x + q_z z)} \quad (22)$$

The linear response function is then

$$\delta\phi(x, y, z) = \sum_{q_x, q_z} f_{q_x, q_z}(y) e^{i(q_x x + q_z z)} \quad (23)$$

Because  $f$  and  $\sigma$  are real functions,  $f_{-q_x, -q_z} = f_{q_x, q_z}^*$  and similarly for  $\sigma$ . The above form enables us to carry out the integration of the free energy in the  $x$ - $z$  plane. Denoting  $\langle \dots \rangle_{xz}$  as the average in the  $x$ - $z$  plane, one can check, for example, that

$$\langle \phi \nabla^2 \phi \rangle_{xz} = \sum_{q_x, q_z} f_{q_x, q_z} \left( f''_{q_x, q_z} - (q_x^2 + q_z^2) f_{q_x, q_z} \right)^* \quad (24)$$

Defining the in-plane  $q$ -vector  $\mathbf{q}_\parallel \equiv (q_x, q_z)$  and performing the free energy minimization with respect to  $f_{q_x, q_z}^*$ , we see that the functions  $f_{q_\parallel} = f_{q_x, q_z}$  obey the same master equation eq 12 that  $f_q$  previously obeyed, with the only change that  $q^2$  is replaced by  $q_\parallel^2$ . For a BCP in contact with a single surface, the appropriate boundary conditions are

$$f''_{q_\parallel}(0) + (q_0^2 - q_\parallel^2) f_{q_\parallel}(0) = 0$$

$$\frac{\sigma_{q_\parallel}}{h} + \frac{2\tau_s}{h} f'_{q_\parallel}(0) + (q_0^2 - q_\parallel^2) f'_{q_\parallel}(0) + f'''_{q_\parallel}(0) = 0 \quad (25)$$

The solution for  $f_{q_\parallel}$  is analogous to eq 14

$$f_{q_1}(y) = A_{q_1} e^{-k_{q_1} y} + B_{q_1} e^{-k_{q_1}^* y} \quad (26)$$

$$k_{q_1}^2 = q_1^2 - q_0^2 + i\alpha(N\chi_c - N\chi)^{1/2} \quad (27)$$

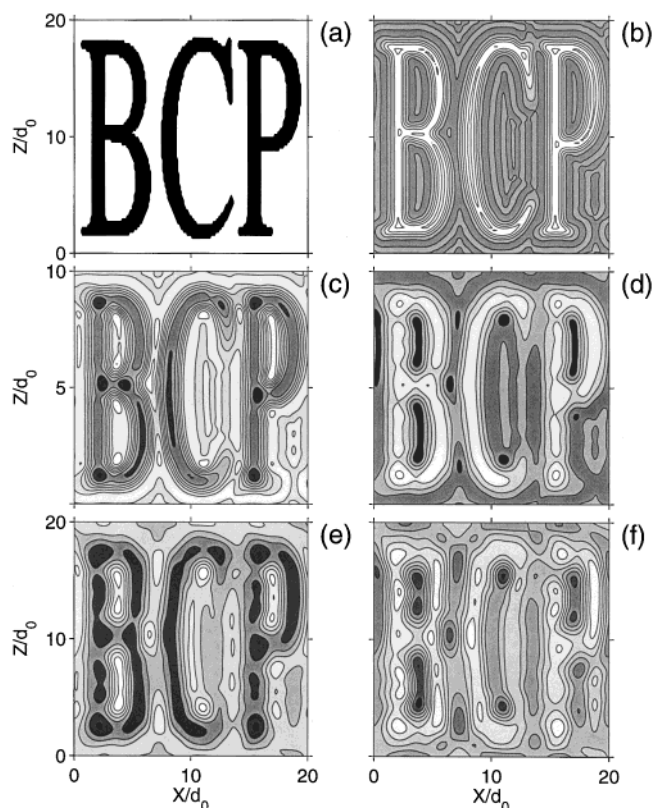
where again  $\alpha \approx 0.59q_0^2$  is a constant. Knowing the response of the polymers to the surface modes  $\sigma_{q_1}$ , one is able to deduce the concentration profiles for any given two-dimensional surface pattern. To illustrate this, we take a system of chemical affinity in the shape of the letters "BCP" on the  $y = 0$  surface (Figure 7a) and calculate the polymer concentration in a sequence of planes parallel and above it. All sizes are expressed in terms of  $d_0 = 2\pi/q_0$ , the fundamental lamellar periodicity. The shape of the letters continuously deforms as one moves away from the surface. Contour plots corresponding to planes parallel to the  $x$ - $z$  surface and separated by a distance  $(n + 1/2)d_0$ , for integer  $n$ , are approximately related to one another by A  $\leftrightarrow$  B interchange of monomers, similar to bulk lamellar systems. Note that parts c and e of Figure 7 are approximately the inverse image ("negative") of parts b, d, and f. The original features are completely washed away as the distance  $y$  from the surface is further increased. In Figure 7 it happens for  $5d_0 \leq y \leq 6d_0$ .

Figure 7 also illustrates circumstances where a certain surface pattern is transferred via the bulk BCP to another surface. It may be important to know, for example, if the contrast of the distant image can be experimentally detected. This reduction of the contrast is clearly seen by comparing Figure 7, parts b and f, and can easily be calculated from our expressions. The lamellar order created parallel to the edges of the letters in Figure 7b is the result of the undulatory nature of the block copolymers: order extending perpendicular to the surface induces order in the direction parallel to it.

When the characteristic pattern size is larger than the polymer length-scale  $d_0$ , the copolymer melt can follow the surface pattern. The effect of reducing the size of the surface structure is seen as a blurred morphology in Figure 8a, where the "BCP" pattern was chosen to have dimensions  $6d_0 \times 6d_0$ , compared to  $20d_0 \times 20d_0$  of Figure 7b. The effect of raising the temperature (further away from the ODT) is seen in Figure 8b. It is similar to Figure 7b, only that the temperature is higher,  $N\chi = 9$ , and the lamellar features along the edges of the letter are less prominent. Again, using our order parameter expressions one can obtain the  $q$ -mode spectrum and contrast of the transferred image, as a function of the original surface pattern  $\sigma(x,z)$ , temperature and distance from the  $y = 0$  surface.

In a thin film, creation of truly three-dimensional, complex morphologies between the two surfaces can be achieved even by using only one-dimensional surface patterns. As an example we choose a simple sinusoidal pattern on each of the  $y = \pm L$  surfaces, rotated  $90^\circ$  with respect to one another:  $\sigma^- = \cos(qx + qz)$  and  $\sigma^+ = \cos(qx - qz)$ . In Figure 9b the resulting morphology in the  $y = 0$  mid-plane is shown and is a superposition of the two surface patterns in parts a and c. Because  $y = 0$  is a symmetric plane, the pattern has a square symmetry. Other patterns are created at different  $y$  planes.

In section III, we showed that the  $q = 0$  mode of the surface pattern is the slowest decaying mode, resulting in a lamellar layering parallel to the surface, and decaying slowly to the bulk value above the ODT as



**Figure 7.** Propagation of surface order into the bulk. In part a is the original chemical pattern (the letters "BCP") at the  $y = 0$  surface, whose size is  $20 \times 20$  in units of  $d_0$ . White corresponds to A-block preferring regions. A sequence of contour plots for  $y = 0.5d_0, 2d_0, 3.5d_0, 5d_0$ , and  $6.5d_0$  is shown in parts b–f, respectively. The original pattern is gradually fading (small features, high  $q$ -modes first) as  $y$  is increased, until it is completely washed out. For  $y \approx (n + 1/2)d_0$  with  $n$  integer, there is an inversion of the original pattern, as the A (light) and B block (dark) are interchanged relative to the original pattern. The Flory parameter is taken as  $N\chi = 9.5$ .

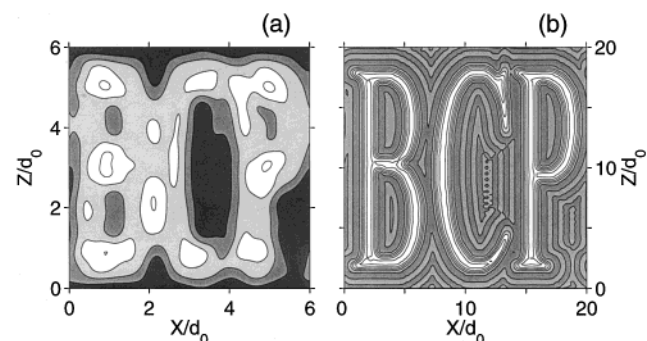


**Figure 8.** Contour plots as in Figure 7b. In part a, the temperature is kept at  $N\chi = 9.5$ , but the surface pattern is reduced to smaller size of about  $6d_0 \times 6d_0$ , while in part b the size is as in Figure 7 but the temperature is higher,  $N\chi = 6$ . The lamellar features along the letter are less prominent than in Figure 7b. Note that the bulk ordering cannot tightly follow the surface pattern when the pattern size becomes comparable to  $1d_0$ , as in part a.

$y \rightarrow \infty$ , no matter what the surface pattern is. We demonstrate this in Figure 10, where in part a we choose a simple one-dimensional structure in the shape of a stripe of width  $d_0$ . Inside the stripe of width  $d_0$ ,  $\sigma(x,z) = 0.5$  while outside it, the surface area is neutral,  $\sigma = 0$ . Thus, the B-polymer is preferentially adsorbed onto the stripe. The order parameter contour plot in the  $x$ - $y$  plane is shown in part b. It can be seen that the

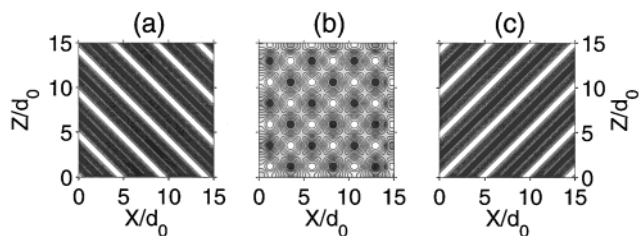


**Figure 9.** Creation of a complex three-dimensional morphology by superposition of two one-dimensional surface patterns:  $\sigma^-(x,z) = \cos(qx + qz)$  and  $\sigma^+(x,z) = \cos(qx - qz)$ . Shown is the thin film BCP morphology, where part a is the surface pattern at the  $y = -L = -d_0$  and part c is the pattern at  $y = L = d_0$ . A contour plot of the order parameter in the mid-plane,  $y = 0$ , is shown in part b, depicting A-rich and B-rich regions with square symmetry. The Flory parameter is taken as  $N\chi = 9$  and  $q = q_0/3$ .

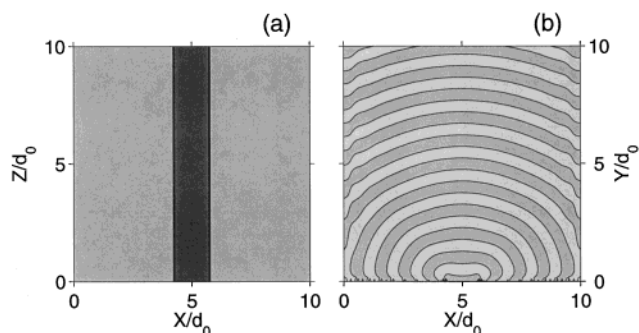


**Figure 10.** Appearance of curved lamellae as a result of a one-dimensional surface pattern along the  $z$  surface axis. In part a, a surface stripe is shown in the  $x-z$  plane. The (black) stripe has a surface field of  $\sigma = 0.5$  inducing preferential adsorption of the B-polymer. The rest of the surface (denoted by a gray color outside the stripe) has  $\sigma = 0$  and is indifferent to A/B adsorption. In part b is a contour plot in the  $x-y$  plane is shown depicting curved lamellae surrounding the middle “disturbance”. As the distance from the stripe is increased more than  $10d_0$  shown here, the lamellae gradually fade away. The Flory parameter is taken to be  $N\chi = 10$ .

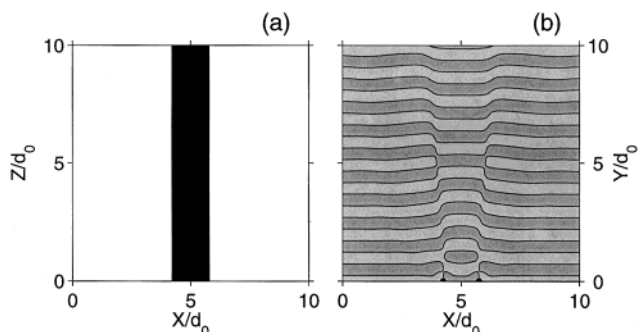


**Figure 11.** Same as in Figure 10, but with  $\sigma = 0.5$  inside the stripe (black), while the rest of the surface (white) has  $\sigma = -0.5$ . In part a, the  $x-z$  surface is shown while in part b the contour plots are shown in the  $x-y$  plane. Far from the stripe, the A-polymer (in light) is adsorbed to the surface, and overall a lamellar morphology parallel to the surface is seen. Close to the stripe disturbance these lamellae are modified, distorted locally by the presence of the stripe.

“surface disturbance” is enclosed with alternating lamellae. The distorted lamellae close to the  $y = 0$  surface appear curved, and slowly fade away as the distance from the surface is increased.

A different scenario is presented in Figure 11, where inside the stripe of thickness  $d_0$ ,  $\sigma = 0.5$  as in Figure 10, but outside the stripe the surface prefers the A monomers:  $\sigma = -0.5$ . We find that the adsorption

the surface is quite different than in Figure 10. Far from the stripe, the A-polymer is adsorbed onto the surface and induces stacking of the BCP in a direction parallel to the surface. Close to the surface perturbation (the stripe) the behavior is altered as the lamellae are strongly deformed in order to optimize their local interaction with the surface stripe.

## V. Conclusions

We have employed a simple Ginzburg–Landau expansion of the BCP free energy to study analytically the interfacial behavior of block copolymers confined by one or two patterned surfaces. Our approach consists of finding the governing equation for a presumably small perturbation to the bulk order parameter, by retaining second-order terms in the free energy. This approach can be justified close to and above the critical point. Above the ODT it gives rise to a simple linear equation with fixed coefficients.<sup>8,18</sup> A generalization to two-dimensional surface patterns is presented, where a complete spatial description of the polymer concentration is given in terms of an arbitrary surface pattern. However, this approach applies to systems below the ODT as well, where a linearization is to be taken around an ordered phase.<sup>36,37</sup>

The assumption that the surface interactions are strictly local means that the length scales of the polymer morphology are determined by bulk properties. Moreover, each of the surface  $q$ -modes in  $\sigma(x) = \sum_q \sigma_q \cos qx$  gives rise to a corresponding mode  $f_q \cos qx$  in the local polymer concentration  $\phi(x,y)$ . This “response” mode is characterized by a single wavevector  $k_q$ . The wavevector  $k_q$  is determined by  $\chi$  and the surface wavenumber  $q$ . In Figure 1 we show the dependence of  $k_q$  on these parameters. The high  $q$ -modes of the surface pattern  $\sigma(x,z)$  decay more rapidly than those of low  $q$ . For high  $q$ -modes of characteristic length scale much smaller than the polymer chains  $d_0$ , the BCP melt cannot follow the surface modulations, and feels just the average of those modulations (which is zero for  $q > 0$ ). This dependence of  $k_q$  on  $q$  and  $\chi$  is similar to the results found by Petera and Muthukumar<sup>18</sup> using a different free-energy functional. Moreover, we generalize surface patterns to any two-dimensional patterns as can be seen in Figure 7. Even within a mode decoupled (linear response) theory, many interesting effects follow for a single surface as well as for films confined between two surfaces.

Our expressions for the spatial dependence of the order parameter on a general patterned surface give a complete description of the system, and allows for the calculation of free energy, pressure, etc. We demonstrate in Figure 9 how the superposition of simple one-dimensional patterns can bring about a three-dimensional behavior in a thin film system. As the pattern propagates in the direction perpendicular to the surface, it also propagates in the direction parallel to it. These considerations, along with tuning the system parameters, may lead to controlled microstructures of BCP confined between two surfaces in various applications. Using a strong enough surface field or working close to the ODT, it may be advantageous to use copolymer films to transfer surface patterns from one surface to another.

**Acknowledgment.** We would like to thank G. Fibich, S. Herminghaus, G. Krausch, M. Muthukumar, R. Netz, G. Reiter, T. Russell, M. Schick, M. Schwartz,

and U. Steiner for useful discussions. Partial support from the U.S.-Israel Binational Foundation (B.S.F.) under Grant No. 98-00429 and the Israel Science Foundation founded by the Israel Academy of Sciences and Humanities—Centers of Excellence Program is gratefully acknowledged.

### References and Notes

- (1) Bates, F. S.; Fredrickson, G. H. *Annu. Rev. Phys. Chem.* **1990**, *41*, 525.
- (2) Ohta, K.; Kawasaki, K. *Macromolecules* **1986**, *19*, 2621.
- (3) Leibler, L. *Macromolecules* **1980**, *13*, 1602.
- (4) Fredrickson, G. H.; Helfand, E. *J. Chem. Phys.* **1987**, *87*, 697.
- (5) Matsen, M. W.; Bates, F. *Macromolecules* **1996**, *29*, 7641.
- (6) Walheim, S.; Schäffer, E.; Mlynek, J.; Steiner, U. *Science* **1999**, *283*, 520.
- (7) Fink, Y.; Winn, J. N.; Fan, S.; Chen, C.; Michel, J.; Joannopoulos, J. D.; Thomas, E. L. *Science* **1998**, *282*, 1679.
- (8) Fredrickson, G. H. *Macromolecules* **1987**, *20*, 2535.
- (9) Tang, H.; Freed, K. F. *J. Chem. Phys.* **1992**, *97*, 4496.
- (10) Turner, M. S.; Rubinstein, M. R.; Marques, C. M. *Macromolecules* **1994**, *27*, 4986.
- (11) Anastasiadis, S. H.; Russell, T. P.; Satija, S. K.; Majkrzak, C. F. *Phys. Rev. Lett.* **1989**, *62*, 1852.
- (12) Menelle, A.; Russell, T. P.; Anastasiadis, S. H.; Satija, S. K.; Majkrzak, C. F. *Phys. Rev. Lett.* **1992**, *68*, 67.
- (13) Shull, K. R. *Macromolecules* **1992**, *25*, 2122.
- (14) Matsen, M. W. *J. Chem. Phys.* **1997**, *106*, 7781.
- (15) Geisinger, T.; Mueller, M.; Binder, K. *J. Chem. Phys.* **2000**, *111*, 5241.
- (16) Pereira, G. G.; Williams, D. R. M. *Phys. Rev. Lett.* **1998**, *80*, 2849. Pereira, G. G.; Williams, D. R. M. *Macromolecules* **1998**, *31*, 5904. Pereira, G. G.; Williams, D. R. M. *Macromolecules* **1999**, *32*, 758.
- (17) Wang, Q.; Nath, S. K.; Graham, M. D.; Nealy, P. F.; de Pablo, J. J. *J. Chem. Phys.* **2000**, *112*, 9996.
- (18) Petera, D.; Muthukumar, M. *J. Chem. Phys.* **1997**, *107*, 9640.
- (19) Petera, D.; Muthukumar, M. *J. Chem. Phys.* **1998**, *109*, 5101.
- (20) Brazovskii, S. A. *Sov. Phys. JETP* **1975**, *41*, 85.
- (21) Fredrickson, G. H.; Binder, K. *J. Chem. Phys.* **1989**, *91*, 7265.
- (22) Binder, K.; Frisch, H. L.; Stepanow, S. *J. Phys. II* **1997**, *7*, 1353.
- (23) Podneks, V. E.; Hamley, I. W. *JETP Lett.* **1996**, *64*, 617.
- (24) Gompper, G.; Schick, M. *Phys. Rev. Lett.* **1990**, *65*, 1116.
- (25) Tsori, Y.; Andelman, D.; Schick, M. *Phys. Rev. E* **2000**, *61*, 2848.
- (26) Netz, R. R.; Andelman, D.; Schick, M. *Phys. Rev. Lett.* **1997**, *79*, 1058.
- (27) Villain-Guillot, S.; Netz, R. R.; Andelman, D.; Schick, M. *Physica A* **1998**, *249*, 285. Villain-Guillot, S.; Andelman, D. *Eur. Phys. J. B* **1998**, *4*, 95.
- (28) Andelman, D.; Brochard, F.; Joanny, J.-F. *J. Chem. Phys.* **1987**, *86*, 3673.
- (29) Garel, T.; Doniach, S. *Phys. Rev. B* **1982**, *26*, 325.
- (30) Shi A.-C. *J. Phys. Condens. Matter* **1999**, *11*, 10183.
- (31) Kellogg, G. J.; Walton, D. G.; Mayes, A. M.; Lambooy, P.; Russell, T. P.; Gallagher, P. D.; Satija, S. K. *Phys. Rev. Lett.* **1996**, *76*, 2503.
- (32) Mansky, P.; Russell, T. P.; Hawker, C. J.; Mayes, J.; Cook, D. C.; Satija, S. K. *Phys. Rev. Lett.* **1997**, *79*, 237.
- (33) Kielhorn, L.; Muthukumar, M. *J. Chem. Phys.* **1997**, *111*, 2259.
- (34) Jacobs, A. E.; Mukamel, D.; Allender, D. W. *Phys. Rev. E* **2000**, *61*, 2753.
- (35) Gido, S. P.; Thomas, E. L. *Macromolecules* **1994**, *27*, 6137.
- (36) Tsori, Y.; Andelman, D. *Europhys. Lett.*, in press, **2001**.
- (37) Tsori, Y.; Andelman, D. Submitted to *J. Chem. Phys.* **2001**.

MA001222K